Contribution from the Department of Chemistry,
Stanford University, Stanford, California 94305

Interactions of the Ruthenium(III)–Ruthenium(II) Couple with Malononitrile and Related Ligands

H. KRENTZIEN and H. TAUBE*

Received January 29, 1982

When dicyanamide and tricyanomethane act as bridging groups in binuclear pentaammineruthenium species, the bridging groups remain anionic over wide pH ranges. When malononitrile, *tert*-butylmalononitrile, and ethylmalononitrile are the bridging groups, the behavior is complicated by proton dissociation from the bridging ligand and instability of the mixed-valence form after proton dissociation. Electrochemical studies have led to estimates of the pK_a values for [3,L,3] and [3,L,2] for the first two ligands. These are −4.8 and −0.7 for L = malononitrile and −3.0 and 1.6 for L = *tert*-butylmalononitrile. In the [2,L,2] states only lower limits on pK_a were set, and these are 13 and 15 for malononitrile and *tert*-butylmalononitrile, respectively. The pK_a values of the free ligand are 11.2 and 13.1. The enormous enhancement of acidity when the nitrile is coordinated to $(NH_3)_5Ru^{III}$ is shown also in the mononuclear *tert*-butylmalononitrile complex, where pK_a was observed to be 3.85, here with use of a spectrophotometric method. The most striking feature of the UV–visible spectra is the strong absorption at high wavelengths shown by the anion–Ru(III) unit. For the [3,L⁻,3] species the values of λ_{max} (ϵ) are (units of nm and M^{-1} cm^{-1}, respectively) 784 (2.8×10^4), 695 (1.7×10^4), 562 (4.5×10^3), and 400 (2×10^3) for the *tert*-butylmalononitrile, malononitrile, tricyanomethanide, and dicyanamide anions, respectively. For the same bridging ligands, the characteristics of the near-IR absorption of the mixed-valence species are 1170 (1.6×10^4), 1280 ($>10^4$), 1550 (6.2×10^3), and 1100 (2.8×10^3). The quotients governing the comproportionation equilibrium [3,L⁻,3] + [2,L⁻,2] = 2[3,L⁻,2] for the same four bridging ligands are $>10^{10}$, $>10^{11}$, 2.3×10^3, and 2×10^2, respectively. These data and other properties such as the width of the near-IR band at half-height suggest that the mixed-valence species based on the anions of *tert*-butylmalononitrile and malononitrile are strongly delocalized but that with the dicyanamide anion as bridging group the systems are valence trapped. When the lone electron pair of the central atom in the bridging group, which mainly appears to account for the coupling in the malononitrile anions, is engaged, as for example when dibenzylmalononitrile is the bridging group, coupling is very weak. This is evidenced by the small value (1.6×10^2 M^{-1} cm^{-1}) of ϵ for the near-IR band in the corresponding mixed-valence species as well as the small value ($\sim$10) for the comproportionation constant.

In the mixed-valence molecules based on the Ru(II)–Ru(III) couple with pyrazine,[1] dicyanogen,[2] and 4,4′-bipyridine[3] as the bridging groups and ammonias as the auxiliary ligands, the π^* orbitals of the bridging groups have been taken[4] as providing the major means of communication between the metal ions. In the mixed-valence molecule based on the anions of malononitrile or *tert*-butylmalononitrile as bridging groups, a different mechanism appears to be dominant, involving delocalization from a π orbital of the ligand to the d orbital of ruthenium(III). A preliminary report of observations with bridging ligands of this kind has been published.[5,6] In this paper, the earlier report is amplified and results with related ligands are described.

Glossary of abbreviations: BYMN, benzylidenemalononitrile; DBMN, dibenzylmalononitrile; *t*-BuMN, *tert*-butylmalononitrile (ion, *t*-BuMN⁻); DCA, acid derived from dicyanamide (ion, DCA⁻); EtMN, ethylmalononitrile (ion, EtMN⁻); MN, malononitrile (ion, MN⁻); TCM⁻, tricyanomethanide ion.

Experimental Section

General Considerations. The procedures for the preparation of air-oxidizable species, which include all of the Ru(II) compounds that will be dealt with in this report, have been described.[7]

Tap distilled water, redistilled from alkaline permanganate, was used throughout.

Buffer solutions were prepared according to standard procedures.[8,9] Alkali-metal chlorides were added to adjust the ionic strength.

Trifluoromethanesulfonic acid was purified by distillation under reduced pressure. The distillate was diluted to approximately 7–8 M and stored in the refrigerator. Ammonium hexafluorophosphate, purchased from Ozark-Mahoning Co. as 99.5% pure reagent, was used as supplied. Iron(III) trifluoromethanesulfonate solution was prepared by adding 1.40 g of reagent grade iron to 100 mL of 2.5 M HSO_3CF_3. The mixture was heated on a steam bath until the metal had almost disappeared, whereupon it was filtered and kept in the refrigerator for 30 min. A 10-fold excess of 30% H_2O_2 was then added dropwise to the solution in an ice bath. After the peroxide had been added, the solution was brought to room temperature and finally heated on a steam bath for 30 min. It was cooled to room temperature and diluted to 250 mL. The solution was standardized by reducing Fe(III) to Fe(II) with hydroxylamine hydrochloride, with Fe(II) being determined spectrophotometrically as $Fe(o\text{-phen})_3^{2+}$.[10]

Organic Chemicals. Sodium dicyanamide was purchased from Aldrich Chemical Co. or Eastern Kodak and was used as supplied. Potassium tricyanomethanide was prepared according to the method of Trofimenko et al.[11] Malononitrile, benzylidenemalononitrile ($C_6H_5CH{=}C(CN)_2$), and the monosubstituted malonic esters needed for the preparation of the corresponding malononitriles were purchased from Aldrich Chemical Co. Ethylmalononitrile was prepared from the corresponding ester by following the procedure described by Russell.[12] *tert*-Butylmalononitrile was prepared from malononitrile with use of the Friedel–Crafts alkylation of Bold et al.[13] The disubstituted derivatives were synthesized from malononitrile according to the method of Bloomfield.[14]

Precursor Ruthenium Compounds. Chloropentaammineruthenium(III) chloride and aquopentaammineruthenium(III) trifluoromethanesulfonate were precursors to other ruthenium compounds. The former was prepared according to the method of Vogt et al.[15] The latter compound was obtained by dissolving [Ru(N-

(1) Creutz, C.; Taube, H. *J. Am. Chem. Soc.* **1969**, *91*, 3988; **1973**, *95*, 1086.
(2) Tom, G. M.; Taube, H. *J. Am. Chem. Soc.* **1975**, *97*, 5310.
(3) Tom, G. M.; Creutz, C.; Taube, H. *J. Am. Chem. Soc.* **1974**, *96*, 7823.
(4) Taube, H. *Ann. N.Y. Sci.* **1978**, *313*, 481.
(5) Krentzien, H. J.; Taube, H. *J. Am. Chem. Soc.* **1976**, *98*, 6379.
(6) Many of the observations made with dicyanamide ion as bridging ligand are described in a separate publication: Sutton, J. E.; Krentzien, H.; Taube, H. *Inorg. Chem.* **1982**, *21*, 2842.
(7) See, for example: Kuehn, C. G.; Taube, H. *J. Am. Chem. Soc.* **1976**, *98*, 689.
(8) Clark, W. M.; Lubs, H. A. *J. Biol. Chem.* **1916**, *25*, 479.
(9) Calowisk, S. P., Kaplan, N. O., Eds. "Methods in Enzymology"; Academic Press: New York, 1955; Vol. 1, p 138.
(10) Charlot, G. "Colorimetric Determination of the Elements"; American Elsevier: New York, 1964; p 274.
(11) Trofimenko, S.; Little, E. L.; Mower, H. F. *J. Org. Chem.* **1962**, *27*, 433.
(12) Russell, P. B. *J. Am. Chem. Soc.* **1950**, *72*, 1853. Russell, P. B.; Hitchings, G. *Ibid.* **1952**, *74*, 3443.
(13) Bold, P.; Militzer, H.; Thielacke, W.; Schulz, L. *Justus Liebigs Ann. Chem.* **1968**, *718*, 101.
(14) Bloomfield, J. J. *J. Org. Chem.* **1961**, *26*, 4112.

0020-1669/82/1321-4001$01.25/0

$H_3)_5OH]S_2O_6$ (this was prepared according to a procedure of Gleu and co-workers)[16] in a minimum of warm 3 M HSO_3CF_3 but keeping the pH below 1. The solution was filtered, an equal volume of 8 M HSO_3CF_3 was added to the filtrate, and when the filtrate was cooled in the refrigerator, an off-white solid formed. This was collected, washed with ether, and vacuum-dried. The yield of $[Ru(NH_3)_5O-H_2](SO_3CF_3)_3$ exceeded 90%.

Mononuclear Ruthenium Pentaammine Complexes. The pentaammineruthenium(II) complexes of dicyanamide, malononitrile, and ethylmalononitrile were obtained by adding 7.0 mmol of the ligand to 5–10 mL of a deareated solution containing 0.35 mmol of $[Ru(NH_3)_5Cl]Cl_2$ or $[Ru(NH_3)_5OH_2](SO_3CF_3)$ at pH 2–3. The solution was reduced under argon, with Zn amalgam, and after 2 h, the solution was filtered under argon. When 1–2 mL of saturated NH_4PF_6 was added, the salts of composition $[Ru(NH_3)_5L](PF_6)_2$ (where L represents the hetero ligand) precipitated. The solid was collected, washed several times with ethanol and ether, and vacuum-dried. The yields were better than 85%.

For L = *tert*-butylmalononitrile and dimethylmalononitrile, 9 mmol of ligand was added to 10 mL of a deareated solution containing 0.3 mmol of $[Ru(NH_3)_5OH_2](SO_3CF_3)_3$ in a 1:1 mixture of aqueous 0.1 M HSO_3CF_3 and ethanol. The resulting solution was deaerated with argon for 10 min, zinc amalgam was added, and the reaction was continued for 2 h under argon. The solution was filtered in an inert atmosphere, and when 2–3 mL of a deaerated saturated solution of NH_4PF_6 in a 1:1 mixture of aqueous 0.10 M HSO_3CF_3 in ethanol was added, the desired product precipitated. The solid was treated as described above. The yield of product exceeded 83%.

For the preparation of dibenzylmalononitrile three drops of 1 M HSO_3CF_3 were added to a deaerated solution of 0.23 mmol of $[Ru(NH_3)_5OH_2](SO_3CF_3)_3$ and 4.5 mmol of L in 10 mL of ethanol. The solution was reduced for 2 h with Zn amalgam under argon and then was filtered in an inert atmosphere. Five milliliters of a saturated solution of NH_4PF_6 in ethanol that contained two drops of 3 M HSO_3CF_3 was then added to the filtrate. The solid was collected and treated as described above.

The ruthenium(II) complex of tricyanomethanide ion was not obtained in pure form, but a satisfactory sample of the ruthenium(III) salt was prepared. The procedure to be described also served for the preparation of the ruthenium(III) complex of dicyanamide. A solution of $[Ru(NH_3)_5H_2O](SO_3CF_3)_3$ (0.40 mmol in 10 mL of 0.01–0.001 M HSO_3CF_3) was warmed to 50–60 °C in a water bath while it was being aspirated with argon. A 10–20-fold excess of ligand was added, and reaction was continued for 3 h, after which the solution of NH_4PF_6 was added. When DCA^- is the ligand, the solid that forms is red-orange, while the TCM^-, it is blue. The solid was collected and treated as described for other preparations. The yield exceeded 70%.

Solid $[Ru(NH_3)_5(MN^-)](PF_6)_2$ was prepared by oxidizing a warm solution containing 0.08 mmol of the ruthenium(II) compound in 2.5 mL of 0.01 M HCO_2CF_3 with a stoichiometric amount of a solution of 0.1 M of ferric chloride. A 10% excess was then added, and the solution was left under argon for 5–10 min. A saturated solution of NH_4PF_6 in 0.1 M HCO_2CF_3 (2–4 mL) was added, and the solid was collected and treated as described above.

Binuclear Pentaammineruthenium Complexes (of DCA, TCM, MN, ETMN, *t*-BuMN). To a solution containing either 0.8 mmol of $[Ru(NH_3)_5Cl]Cl_2$ or $[Ru(NH_3)_5OH_2](SO_3CF_3)_3$ in 10 mL of H_2O at pH 2–3 was added 0.4 mmol of the desired ligand. The solution was deaerated for 10 min and then reduced for 3 h under argon, with zinc amalgam. The solution was filtered in an inert atmosphere, and 2 mL of a deaerated saturated solution of NH_4PF_6 in 0.1 M HCO_2CF_3 was then added. The solid binuclear complex was collected and treated as described above. When the ligand proved to be incompletely soluble in the reaction mixture, enough ethanol was added to bring it into solution. For dibenzylmalononitrile, the reaction medium was ethanol.

The bis(ruthenium(III)) complexes with MN, *t*-BuMN, EtMN, and TCM were prepared from the corresponding bis(ruthenium(II)) complexes with Fe(III) as oxidizing agent. A 10–15% excess of Fe(III) was added to 10 mL of a reaction solution containing 0.08 mmol of the bis(ruthenium(II)) form, followed after 10 min by addition of 3–5 mL of a saturated solution of NH_4PF_6 in 0.1 M HCO_2CF_3. The solid was collected and treated as described for other preparations.

Apparatus and Methods. Ultraviolet and visible absorption spectra were recorded with a Cary 15, Cary 14, or Beckman Acta MVII spectrophotometer, with near-infrared spectra taken on either of the last two instruments. Infrared spectra were recorded on a Perkin-Elmer 621 grating spectrophotometer covering the range 4000–250 cm^{-1}.

For magnetic susceptibility measurements, a Model 7600 Cahn Faraday apparatus was used. The susceptibility standard was $HgCo(SCN)_4$. Diamagnetic corrections were applied with use of published tables.[17]

Cyclic voltammetry measurements were made with an apparatus constructed by G. Tom and modified by G. M. Brown.[18] Cyclic voltammograms were recorded on an Omnigraphic 200 X-Y recorder with type 5 and 6 precision attenuators (purchased from Houston Instruments). Scan rates for routine cyclic voltammetry were of the order of 50–200 mV/s.

A standard calomel electrode (SCE) was used as the reference, and the potentials were corrected to the normal hydrogen electrode (NHE) by adding 0.242 V to the measured potential. The auxiliary electrode was a piece of platinum wire, and the indicator electrode was a platinum bead sealed in glass, a carbon paste electrode, or a hanging mercury electrode purchased from Brinkman Instruments (Model E410). The concentration of the solution used was at least 0.5 mM, and the supporting electrolyte was at least 0.1 M.

Formal potentials for reversible couples were taken as the mean of the anodic and cathodic peaks. For each measurement the electrodes were checked and corrections for the junction potential were applied by standardization using known couples such as $Ru(NH_3)_6^{3+,2+}$ or *cis*-$Ru(NH_3)_4(isonicotinamide)_2^{3+,2+}$.

Potentiometric Titrations. Potentiometric titrations were done whenever cyclic voltammetry could not be used owing to adsorption problems or irreversible behavior arising from slow deprotonation. Typically about 5 mL of a buffered solution about 1.0×10^{-3} M in the species being studied was titrated with an oxidizing agent compatible with the buffer mixture. The potential was measured with a Metrohm 101 pH meter and the Pt-wire–SCE combination of the CV cell. A Gilmont micrometer syringe was used to dispense the oxidizing solutions. When the potential drifted because of secondary reactions, it was read as a function of time and the correct potential was taken as the extrapolated zero-time value.

Most values of pK_a were determined electrochemically, but on occasion spectrophotometry was used. Titrations were made using an apparatus for continuous monitoring fitted with a Metrohm microcombination electrode on top, a Gilmont micrometer syringe on the side arm, and a 1-cm cell. The pH and spectra were recorded after each addition, and the value of the pK_a was determined by using the relationship

$$pK_a = pH + \log \frac{A' - A}{A - A^\circ}$$

where A', A°, and A refer respectively to the absorbances of the fully protonated ligand complex, deprotonated ligand complex, and the mixture at a given pH. If either A' or A° is unknown, the value of the pK_a could be determined from the slope of the plot A vs. $(A' - A)[H]^+$ or A vs. $[H^+]/(A - A^\circ)$, or by a plot of the absorbance vs. pH at a given wavelength.

Microanalyses were performed by the Stanford Microanalytical Laboratory.

Analyses of the compounds critical for the studies to be described are summarized in Table I.

Results

1. Electrochemical and Related Properties. For mononuclear and for some of the binuclear species, the electrochemical behavior was straightforward, and cyclic voltammetry sufficed to fix the values of the formal potentials, E_f. The results of the measurements are summarized in Table II (first eight entries). However, the binuclear species based on malononitrile and other derivatives having dissociable protons show quite complicated electrochemical behavior, and the results for these systems will be enlarged upon.

(15) Vogt, L. H.; Katz, J. L.; Wiberly, S. E. *Inorg. Chem.* **1965**, *4*, 1157.
(16) Gleu, K.; Breuel, K. *Z. Anorg. Allg. Chem.* **1938**, *237*, 335. Gleu, K.; Buddecker, I. *Ibid.* **1952**, *268*, 202.
(17) Earnshaw, A. "Introduction to Magnetochemistry"; Academic Press: New York, 1919; p 22.
(18) Tom, G. M. Ph.D. Thesis, Stanford University, 1975.

Table I. Microanalytical Results

	element	% calcd	% obsd
$[Ru(NH_3)_5(TCM^-)](PF_6)_2 \cdot 4H_2O$	C	7.53	7.63
	H	3.63	2.45
	N	17.56	17.59
	Ru	15.83	15.80
$[(Ru(NH_3)_5)_2(TCM^-)](PF_6)_5$	C	4.05	4.58
	H	2.55	2.65
	N	15.33	14.83
	Ru	17.02	17.30
$[Ru(NH_3)_5(MN^-)](PF_6)_2$	C	6.65	6.86
	H	3.16	3.12
	N	18.08	18.45
$[(Ru(NH_3)_5)_2(MN)](PF_6)_4$	C	3.54	3.68
	H	3.11	3.17
	N	16.50	16.77
$[(Ru(NH_3)_5)_2(MN^-)](PF_6)_5$	C	3.10	3.49
	H	2.69	2.76
	N	14.46	14.66
	Ru	17.40	17.60
$[(Ru(NH_3)_5)_2(MN^-)]Br_5$	C	4.30	4.66
	H	3.74	3.67
	N	20.08	19.96
	Ru	24.15	24.10
$[Ru(NH_3)_5(t\text{-BuMN})](PF_6)_2$	C	14.05	14.05
	H	4.21	4.21
	N	16.39	16.29
	Ru	16.89	16.90
$[(Ru(NH_3)_5)_2(t\text{-BuMN})](PF_6)_4$	C	7.82	8.23
	H	3.75	3.66
	N	15.64	15.33
	Ru	18.81	18.90
$[(Ru(NH_3)_5)_2(DBMN)](PF_6)$	C	17.00	17.34
	H	3.70	3.76
	N	14.00	13.30
$[(Ru(NH_3)_5)_2(BYMN)](PF_6)_4$	C	10.85	10.13
	H	3.37	3.21
	N	15.18	15.12

Table II. Summary of Electrochemical Results (V)[a]

species	E_f[b]	E_f'
$[(NH_3)_5Ru(DCA^-)]$	0.15	
$[((NH_3)_5Ru)_2(DCA^-)]^{5+,4+,3+}$[c]	0.26[d]	0.11
$[(NH_3)_5Ru(TCM^-)]^{2+,1+}$[c]	0.30	
$[((NH_3)_5Ru)_2(TCM^-)]^{5+,4+,3+}$[c]	0.44[d]	0.24
$[(NH_3)_5Ru(MN)]^{3+,2+}$[c]	0.57	
$[(NH_3)_5Ru(EtMN)]^{3+,2+}$[c]	0.56	
$[(NH_3)_5Ru(t\text{-BuMN})]^{3+,2+}$[c]	0.58	
$[((NH_3)_5Ru)_2(DBMN)]^{6+,5+,4+}$[d]	0.65	0.60
$[((NH_3)Ru)_2(MN)]^{6+,5+,4+}$[e]	(0.63)	(0.57)
$[((NH_3)_5Ru)_2(t\text{-BuMN})]^{6+,5+,4+}$[e]	(0.63)	(0.57)
$[((NH_3)_5Ru)_2(MN^-)]^{5+,4+,3+}$[f]	0.39	<−0.25
$[((NH_3)_5Ru)_2(t\text{-BuMN}^-)]^{5+,4+,3+}$[f]	0.36	<−0.23

[a] At 25 °C in 0.10 M HCl, except where otherwise noted. [b] E_f refers to the first stage of reduction and E_f' to the second. [c] From cyclic voltammograms showing reversible behavior: Peak to peak separation in the range 60–70 mV; sweep rate 50–200 mV/s. [d] Invariant in the pH range 1–7. [e] See text for assumptions on which these are based. [f] See text.

One difficulty stems from the tendency of the malononitrile species to adsorb on the electrodes. As a result, only first scans were considered in the cyclic voltammetric results, and the auxiliary and indicator electrodes were pretreated after each measurement by cleaning or surface renewal. In addition there are intrinsic complications which arise from the proton dissociation of the coordinated ligands. Spectrophotometric investigations show that the [3,MN,3] species does not change its state of protonation in the pH range $1 \leq pH \leq 5$ (above pH 5, nitrile hydrolysis becomes rapid), and the [2,MN,2] species shows no change in the range $1 \leq pH \leq 12.7$. The observations are compatible with the electrochemical results if MN in the [3,3] species is present as the ion above pH 1

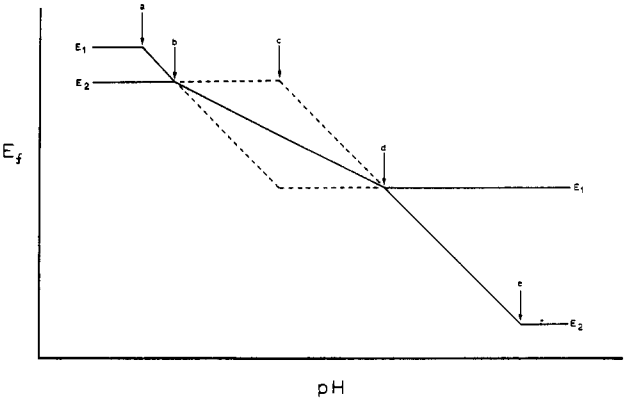

Figure 1. Schematic diagram of the electrochemical behavior of the system [3,L,3]–[3,L,2]–[2,L,2], where L has a dissociable proton. It is understood that the experimental points will not show the sharp breaks that appear in the schematic.

and if the species [2,MN,2] does not undergo acidic dissociation below pH 12.7. The values of pK_a for the free ligands MN and *t*-BuMN are reported as 11.19 and 13.10, respectively.[19]

Figure 1 shows the equilibrium behavior (E vs. pH) that can be expected for systems of the kind we are dealing with. It is assumed that the pK_a values are in the order [3,3] < [3,2] < [2,2], an assumption that is reasonable and that moreover is borne out by the results. In the discussion immediately following, E_1 will refer to the [3,3]–[3,2] couple and E_2 to the [3,2]–[2,2], in each case regardless of the state of protonation (the values of E_f as used in Table II are pH independent while E_1 and E_2 can vary with pH).

Below pH = *a* (see Figure 1), all forms are protonated, and in this regime the two half-reactions are as shown by eq 1 and 2. Owing to the high acidity of [3,L,3] this regime is not

$$[3,L,3] + e^- = [3,L,2] \quad (1)$$

$$[3,L,2] + e^- = [2,L,2] \quad (2)$$

directly accessible for the ligands of present interest. The behavior in this range, however, is approximated by using data for malononitriles that cannot undergo proton dissociation. The electrochemistry of such systems shows that the comproportionation constant for the reaction of [3,3] with [2,2] to form 2[3,2] is small, ~10 for the case of $[((NH_3)_5Ru)_2(DBMN)]$, and it will be assumed to be 10 also for the protonated malononitriles. The pH at *a* corresponds to the pK_a for the acid dissociation of [3,L,3], and at higher pH, half-reaction 2 is replaced by (3). Above pH = *a*, E_1 then decreases

$$[3,L^-,3] + H + e^- = [3,L,2] \quad (3)$$

at the rate of 59.2 mV/pH unit, but since in this range neither [3,L,2] nor [2,L,2] yields H^+, E_2 remains constant. At point *b*, E_1 has dropped to the value of E_2, and as the pH increases further, the mixed-valence species becomes unstable with respect to disproportionation. If equilibrium is maintained, the net half-reaction now is shown by eq 4, and the measured value

$$[3,L^-,3] + H^+ + 2e^- = [2,L,2] \quad (4)$$

of E will correspond to the solid line, which has a slope of 29.6 mV/pH unit. If E_1 and E_2 could be measured in the pH region between *c* and *d*, they would follow the lower and upper dotted lines, respectively, where the pH at *c* corresponds to the pK_a for [3,L,2]. Below this pH, E_2 decreases with a slope of 59.2 mV/pH unit while E_1 remains constant. As a consequence, the [3,2] state becomes stable above pH = *d* and thus separate

(19) Hibbert, F.; Long, F. A. *J. Am. Chem. Soc.* **1971**, *93*, 2829, 2836.

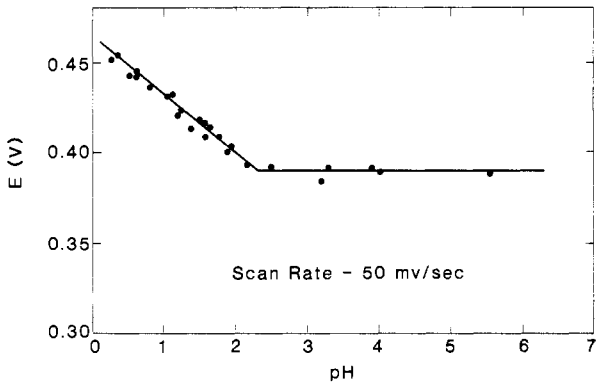

Figure 2. Acid dependence of E for the $[((NH_3)_5Ru)_2(MN)]$ complex as measured by cyclic voltammetry.

redox stages should be observed at pH $>d$ corresponding to half-reactions 5 and 6, where E_2 but not E_1 is pH dependent.

$$[3,L^-,3] + e^- = [3,L^-,2] \quad (5)$$

$$[3,L^-,2] + H^+ + e^- = [3,L,2] \quad (6)$$

Finally, if the pK_a for [2,L,2] is equal to e, above this pH, E_2 now also becomes independent of pH.

In an exploration of the electrochemical behavior, cyclic voltammetry results were of unlimited use, but those obtained for the complex with MN as bridging group do yield some information and will be outlined.

Starting at low pH, the peak-to-peak separation increased with pH, the reduction peak moving to progressively lower potentials while the oxidation peak remained constant at ca. 0.28 V vs. NHE. The change in the reduction peak with pH is shown in Figure 2. In the range where E changes with pH, the slope corresponds approximately to $2e/H^+$ (33 mV/pH unit compared to 29.6 mV/pH unit theoretical). Application of the Randles–Sevcik equation[20] using $[(NH_3)_5Ru(py)H]^{3+/2+}$ as reference gave for n the value 1.72. The net change in the pH region below the break in Figure 2 can therefore be represented by eq 7. If protonation on reduction is rapid, but

$$[3,MN^-,3] + H^+ + 2e^- = [2,MN,2] \quad (7)$$

deprotonation is slow, the general behavior is accounted for. Protonation of the anions of free malononitrile is known to be rapid—$k \approx 10^8$–10^9 M^{-1} s^{-1}—while deprotonation is slow—k in the range (1.4×10^{-2})–(5.4×10^{-4}) s^{-1}.[19] Deprotonation of [2,MN,2] may well be even slower than that of the free ligands (vide infra). Oxidation in the system thus involves electron withdrawal from [2,MN,2] without benefit from deprotonation. Though deprotonation is not rapid enough to make the electrochemical behavior reversible in the CV time scale, it is rapid enough to ensure that after oxidation [3,L,3] is produced by the time the sweep enters the reduction phase. Measurement of the deprotonation rate for [3,L,3] by a stopped-flow spectrophotometric method using Fe(III) to oxidize [2,L,2] fixed $t_{1/2}$ as <5 ms (for this experiment, $[Ru(II)] = 1 \times 10^{-4}$ M, Fe^{3+} in 20–30-fold excess, and [HCl] = 0.10 M). On the other hand, since protonation is rapid, the reduction wave shows a nearly theoretical pH dependence.

The data shown in Figure 2 conform to the ideal scheme shown in Figure 1 if the break in the line is identified with d. The horizontal portion then represents half-reaction 5.

In view of the irreversibility of the CV traces, an effort was made to extract the electrochemical parameters by potentiometric titrations. In Figure 3 the values of E for the 50%

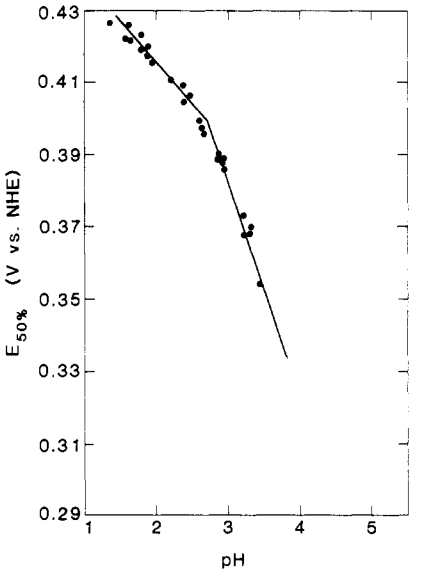

Figure 3. Acid dependence of the potential at 50% oxidation for the $[((NH_3)_5Ru)_2(MN)]$ complex.

oxidized samples of [2,MN,2] at $\mu = 0.1$ and 25 °C are shown as a function of pH. Here again difficulties were encountered, now with slowly drifting potentials ascribable to hydration of the nitrile coordinated to Ru(III) and to other decomposition reactions. The data represent a compromise between waiting for the normal stabilization of potentials and minimizing the effect of decomposition. Below pH 2.7, where there is a break in the curve, the slope of E vs. pH is ca. 25 mV/pH unit, in approximate agreement with the CV data in the same range, again indicating that reaction 4 represents the net half-reaction in this range.

Owing to the decomposition of the mixed-valence species (vide infra) the potentiometric data are of little utility in defining equilibrium stability. They are reassuring to the extent that, in the pH region where the mixed-valence species disproportionates to the isovalent forms, the data agree reasonably well with those obtained by cyclic voltammetry. If the system were ideal in behavior, and stoichiometry were exact, there should be no break in the plot of potential vs. pH at the point d. Below d, the mixed-valence species becomes the dominant form and is in equilibrium with equal concentrations of the [2,2] and the [3,3] species, and any slight deviation from ideal stoichiometry would produce large changes in the measured potential. The break that is observed then shows that the average oxidation state for the ruthenium is below that corresponding to the [3,2] state and therefore that some decomposition has occurred. Because of the uncertainty in the meaning of this break, we prefer to use the break in the cyclic voltammetric data as better defining the thermodynamic parameters.

Starting then with a potential of 0.39 V at a pH of 2.3, using for E_2 the value of E_f for the mononuclear complex, 0.57 V, and using the theoretical slope of 29.6 mV/pH unit rather than the experimental one of 25 mV/pH unit, we calculate the pH at point b to be −3.8. This fixes the pK_a for the mixed-valence species at −0.7 and for the fully oxidized form at −4.8. These estimates of the pK_a values are admittedly rough and may be in error by as much as 2 units. Nevertheless, they seem to show that both the [3,3] and the [3,2] species are very acidic.

If the pK_a for [2,MN,2] were known, the whole diagram of Figure 1 as it pertains to MN as bridging group could be constructed. The spectrophotometric results quoted earlier show that the pK_a in question is greater than ca. 13. An upper limit then to E_f for the half-reaction (8) is −0.25 and this

$$[3,MN^-,2] + e^- = [2,MN^-,2] \quad (8)$$

(20) See, for example: Bard, A. J.; Faulkner, L. R. "Electrochemical Methods"; Wiley: New York, 1980; p 216.

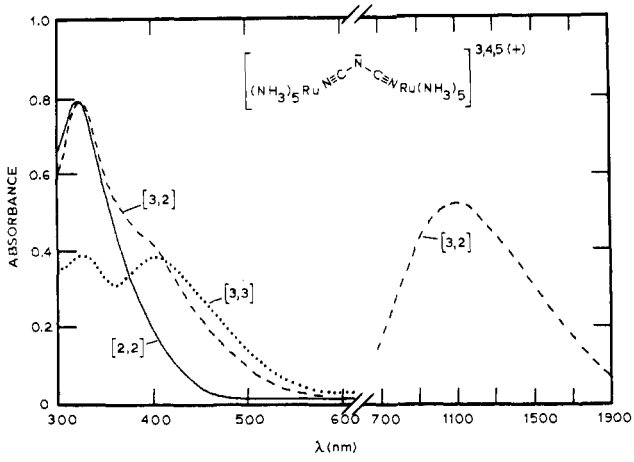

Figure 4. Visible–UV spectra for [3,DCA⁻,3] (dotted line), [3,DCA⁻,2] (dashed line), and [2,DCA⁻,2] (solid line).

together with E_f for the first-stage of reduction places a lower limit on the comproportionation constant for reaction 9 of 10^{11}.

$$[3,MN^-,3] + [2,MN^-,2] = 2[3,MN^-,2] \quad (9)$$

Unfortunately, for the species with *t*-BuMN as the bridging group we gathered only potentiometric data. The curve resembles that in Figure 3, but point *d* is now defined by E = 0.36 and pH 5.1. Since the break in Figure 3 is not much different from that shown in Figure 2, and further that the species [3,*t*-BuMN,2] decomposes less rapidly than [3,MN,2], we will use the quoted values as defining the equilibrium break. On repeating the procedure outlined for the malononitrile system, here again using 0.57 V for E_2, we calculate the value of pK_a for the mixed-valence species as 1.6 and for the fully oxidized form as −3.0. Spectrophotometric studies showed that [2,*t*-BuMN,2] is unaltered at a pH as high as 14, and 15 can be considered a lower limit on pK_a in this case. On this basis an upper limit for E_f corresponding to the reaction (10) is

$$[3,t\text{-BuMN}^-,2] + e^- = [2,t\text{-BuMN}^-,2] \quad (10)$$

−0.23, and $K_{com} > 10^{10}$. Cyclic voltammetry in 3 M HCl produced a wave at 0.46 V, but owing to the difference in medium (μ = 3), the uncertainty associated with the CV data, and possible incomplete protonation, the assumed value of E = 0.57 V for the couple [3,*t*-BuMN,2]–[2,*t*-BuMN,2] is preferred to the "experimental" value.

In connection with the estimates of pK_a values which have been made, it is informative to record the value of pK_a for $[(NH_3)_5Ru(t\text{-BuMN})]^{3+}$ obtained by a spectrophotometric method, using buffers and keeping μ at 1.0. This takes advantage of the fact that only when the ligand is ionized is the species deeply colored (vide infra). The value of pK_a determined in this way is 3.85. If, as we believe, there is considerable stabilization of the mixed-valence species by electron delocalization, a somewhat lower value of pK_a for [3,*t*-BuMN,2] as compared to the value for the mononuclear species is not unreasonable.

2. Ultraviolet–Visible Absorption Spectra. The spectrophotometric results are summarized in Table III. For the binuclear ions based on DCA as bridging group, the spectra are shown in Figure 4, which also includes the absorption in the near-IR for the mixed-valence species. DCA⁻ as a bridging group is exceptional in giving rise to near-IR absorption which is well separated from absorption in the visible region of the spectrum. Also noteworthy is the very intense absorption at long wavelength for the malononitrile anion coordinated to Ru(III).

3. Absorption in the Near-IR. The electrochemical studies showed that to have the mixed-valence species as the dominant forms in half-oxidized solutions of the fully reduced forms, the pH must be above 2.3 for the MN-based system and still higher for the *t*-BuMN species. Conditions were accordingly adjusted for the experiments to be described.

Table III. Visible and UV Spectra[a]

species	λ_{max}, nm (log ϵ)[b]
$[(NH_3)_5Ru(DCA)]^+$	220
$[((NH_3)_5Ru)_2(DCA^-)]^{3+}$	223 (4.4), 325 (35)
$[((NH_3)_5Ru)_2(DCA^-)]^{5+}$	326 (3.4), 400 (3.3)
$[(NH_3)_5Ru(TCM^-)]^{2+}$	237 (4.14), 593 (3.66)
$[((NH_3)_5Ru)_2(TCM^-)]^{3+}$	250 (4.56)
$[((NH_3)_5Ru)_2(TCM^-)]^{4+}$	237 (4.30), 275 sh, 540 (3.65)
$[((NH_3)_5Ru)_2(TCM^-)]^{5+}$	233 (4.24), 562 (3.65)
$[(NH_3)_5Ru(DBMN)]^{2+}$	260 (4.2)
$[((NH_3)_5Ru)_2(DBMN)]^{4+}$	218 sh, 264 (4.45), 320
$[((NH_3)_5Ru)_2(BYMN)]^{4+}$	498
$[(NH_3)_5Ru(MN)]^{2+}$	242 (4.20), 350 sh
$[((NH_3)_5Ru)_2(MN)]^{4+}$	249 (4.44), 350 sh
$[((NH_3)_5Ru)_2(MN)]^{5+}$	225 (4.16), 695 (4.23)
$[(NH_3)_5Ru(EtMN)]^{2+}$	247 (4.19), 350 sh
$[((NH_3)_5Ru)_2(EtMN)]^{4+}$	254 (4.43)
$[((NH_3)_5Ru)_2(EtMn^-)]^{5+}$	786 (4.3)
$[(NH_3)_5Ru(t\text{-BuMN})]^{2+}$	249 (4.28)
$[(NH_3)_5Ru(t\text{-BuMN}^-)]^{2+}$	790 (4.18)[c]
$[((NH_3)_5Ru)_2(t\text{-BuMN})]^{4+}$	255 (4.49) 350 sh
$[((NH_3)_5Ru)_2(t\text{-BuMN}^-)]^{5+}$	220 sh, 282, 784 (4.45)

[a] As hexafluorophosphate salts in 0.1 M HCl or, on occasion, 0.1 M CF_3SO_3H with the exception of $[((NH_3)_5Ru)_2(DBMN)](PF_6)_4$, which was run in acetonitrile. [b] Units for ϵ, M^{-1} cm^{-1}. [c] NaOAc–HOAc, μ = 1 buffer.

The spectra of the half-oxidized ([3,2]) species show bands in the near-IR that are absent from the fully reduced and fully oxidized forms. Oxidations were performed in solution by using $Fe(bpy)_3^{3+}$, *cis*-$Ru(NH_3)_4(isn)_2^{3+}$ [21] or Ce(IV) and by using the [2,2] or [3,3] forms as defining the base line. With DCA, TCM, or DBMN as bridging groups, there are no serious problems with stability (at worst slow nitrile hydrolysis in [3,DBMN,3] and moderately rapid aquation in [2,DCA⁻,2]), but with the MN-, EtMN-, and *t*-BuMN-based species, decay of the oxidized state is quite rapid, at least in water. For example, [3,MN⁻,2] decays on the time scale of seconds in water at 10 °C, and though [3,*t*-BuMN⁻,2] is more stable, the half-time for its decay is on the order of minutes at 25 °C. In all cases, the decomposition reactions are much slower in nonaqueous solvents. Since reasonable data were obtained even in the potentiometric studies described earlier, it seems likely that the rate of decomposition decreases as the pH is lowered.

The data for the mixed valence species are summarized in Table IV.

4. Infrared Spectra. Data for prominent bands that can be rather unambiguously assigned are summarized in Table V.

5. Magnetic Susceptibility. The results of the measurements of magnetic susceptibility are summarized in Table VI.

6. Observations on Decompositions. Experiments were done to follow the changes that occur when $[Ru(NH_3)_5MN]^{2+}$ is oxidized. Iron(III) was used, and the rate of oxidation of $[Ru(NH_3)_5MN]^{2+}$ by Fe^{3+} was measured to facilitate the interpretation of the results. In 0.1 M HCl at 25 °C, the rate constant is 2.5×10^4 M^{-1} s^{-1}, and thus the reaction is rapid enough so that at the concentration levels used in the subsequent experiments we can be certain that the oxidation of Ru(II) to Ru(III) is complete before the processes now to be described take place.

The rate of deprotonation was followed by monitoring the appearance of an absorption at 780 nm, which corresponds

(21) Gaunder, R. G. Ph.D. Thesis, Stanford University, 1969.

Table IV. Near-Infrared Absorption[a]

species	λ_{max} (ϵ) D_2O	CH_3CN	HCON-$(CH_3)_2$	CH_3CON-$(CH_3)_2$	$SO(CH_3)_2$	$(CH_3)_2CO$
[3,DCA^-,2]	1100 (2.8×10^3)	1275	1130	...	1200	1220
[3,TCM^-,2]	1550 (6.2×10^3)	1580	1610	1640	1660	1580
[3,MN^-,2]	1280[b] (>10^4)	1295	1340	...	1370	1270
[3,$EtMN^-$,2]	1170 (>10^4)	1160	1240	1260	1270	1175
[3,*t*-$BuMN^-$,2]	1170 (1.6×10^4)[c]		1160	1260	1275	1170
[3,DBMN,2]	...		990[d]	930	950	930

[a] Units: λ, nm; ϵ, M^{-1} cm^{-1}. [b] 1240 in CH_3OH. [c] At pH 5.0. [d] $\epsilon = 1.6 \times 10^2$.

Table V. Selected Infrared Frequencies[a] (cm^{-1}) for PF_6 Salts

	CN	NH_3	medium
$[(NH_3)_5Ru(DCA^-)]^{2+}$	2300 (s), 2245 (s), 2180 (vs)	1615 (s), 1350 (m), 800 (s)	KBr
$[((NH_3)_5Ru)_2(DCA)]^{5+}$[c]	2300 (s), 2250 (s), 2190 (s)	1620 (s), 1330 (m)	Nujol
$[(NH_3)_5Ru(TCM^-)]^{2+}$[d]	2183 (vs), 2170 (s, sh)	1600 (s), 1400 (m), 793 (m)	CsI
MN	2275 (w), 2268 (s)		KBr
$[(NH_3)_5Ru(MN^-)]^{2+}$	2270 (m), 2252 (w, sh)	1615 (s), 1280 (s)	KBr
$[((NH_3)_5Ru)_2(MN)]^{4+}$	2230 (s), 2205 (sh)	1615 (s), 1275 (s)	KBr
$[((NH_3)_5Ru)_2(MN^-)]^{5+}$	2210 (w, sh), 2165 (s), 2135 (s)	1605 (s), 1295 (s)	KBr
t-BuMN	2270 (w), 2260 (s)		$CHCl_3$
$[((NH_3)_5Ru)_2(t\text{-}BuMN)]^{4+}$	2240 (s)	1630 (s), 1250 (s)	KBr
$[((NH_3)_5Ru)_2(t\text{-}BuMN^-)]^{5+}$	2150 (sh), 2115 (m), 2055 (s)	1625 (s), 1270 (s)	KBr
$[((NH_3)_5Ru)_2(EtMN)]^{4+}$	2240 (s)	1635 (s), 1285 (s)	KBr

[a] The abbreviations v, s, m, w, and sh denote very, strong, medium, weak, and shoulder, respectively. [b] Additional assignments: ν(N-CN) 1390 (m), 900 (s); N-CN def 490 (w), 485 (w); ν(Ru-N) 450. [c] Additional assignments: N-CN def 550, 490; ν(Ru-N) 450. [d] Additional assignments: ν(C-C) 1270 (m).

Table VI. Magnetic Susceptibility of Various Ru(III) Ammines

compd	$10^6\chi$,[a] cgsu/mol	μ, μ_B/mol
$Ru(NH_3)_6Cl_3$	1900	2.13
$[Ru(NH_3)_5Cl]Cl_2$	1928	2.14
$[(Ru(NH_3)_5(TCM^-)](PF_6)_2 \cdot H_2O$	1730	2.03
$[Ru(NH_3)_5(DCA^-)](PF_6)_2$	2016	2.19
$[((NH_3)_5Ru)_2(TCM^-)](PF_6)$	1902	2.12
$[((NH_3)_5Ru)_2(TCM^-)](PF_6)_5$	3430	2.85
$[((NH_3)_5Ru)_2(MN^-)](PF_6)_5$	1290	1.88
$[((NH_3)_5Ru)_2(MN^-)]Br_5$	1720	2.03
$[((NH_3)_5Ru)_2(t\text{-}BuMN^-)](PF_6)_5 \cdot EtOH$	250	0.98

[a] After diamagnetic corrections have been made.

to the maximum in the visible band of $[Ru(NH_3)_5(MN^-)]^{2+}$. The absorption grows in at 25 °C and $\mu = 0.1$ M at a specific rate of 1.06×10^{-1} s^{-1} (25 °C, $\mu = 0.1$ M, pH 2.5). The small increase in rate compound to that for the free ligand—1.43×10^{-2} s^{-1} at 25 °C and $\mu = 0.10$ M[19]—in view of the large increase in acidity attending coordination to Ru(III) is surprising, and it is conceivable that a first-order process after deprotonation was being followed.

Following deprotonation, further changes take place. These have not been worked out in detail, but ion-exchange chromatography has shown a major product to be a species of charge 4+, suggesting that a dimerization occurs.

The stability of the [3,L^-,3] ions in 0.1 M HCl at 25 °C was assessed for L^- = MN^-, $EtMN^-$, and *t*-$BuMN^-$. Iron(III) was used as oxidant, in slight excess to ensure complete oxidation, or the [3,L^-,3] salt was dissolved in the reaction medium. The ions with L^- = MN^- or *t*-$BuMN^-$ were found to be quite stable—$t_{1/2}$ for decomposition >4 h—but the species with L^- = $EtMN^-$ was found to be shorter lived, the lifetime decreasing as the concentration of excess Fe(III) is increased. With *cis*-$[Ru(NH_3)_4(isn)_2]^{3+}$ as oxidant, by taking advantage of the strong absorption band of the 2+ product in the visible region, we demonstrated directly the consumption of excess oxidant. Cyclic voltammetric measurements on the product mixture indicate an amide–Ru(III) bond in the product. (Benzylidenemalononitrile)pentaammineruthenium(III) hydrolyzes rapidly to the corresponding amide complex. A possible reaction sequence for the $EtMN^-$ species consistent with the observations, including the consumption of excess oxidizing agent, is conversion of the ligand to the ylidenemalononitrile

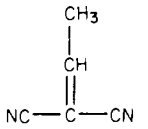

followed by hydrolysis of one of the nitriles to an amide.

When [2,MN,2] is partially oxidized in 0.01 M HCl, μ = 0.1, by Fe(III), so that [2,MN,2] and [3,MN,2] are the dominant species, a process different from any heretofore described takes place. An absorption band with maximum at 760 nm grows in, governed by a rate constant of 1.6×10^{-3} s^{-1} as the near-IR band disappears. The rate is much less for the ethyl and *tert*-butyl derivatives. Hydrolysis of the nitrile to amide cannot of itself account for the development of the color. It is possible that linkage isomerization to produce

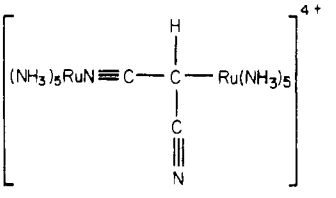

is taking place, with intervalence absorption in the unsymmetrically bound Ru(II)–Ru(III) centers accounting for the absorption at 760 nm.

Discussion

Each of the anionic ligands dealt with in this study offers the central atom and the CN groups as potential binding sites, and the issue of the structures of the complexes must be dealt with. The cyclic voltammetry results reveal no complications ascribable to linkage isomerization (cf. Table II, data for

DCA^- and TCM^-), and since it is unlikely that such isomerization would be more rapid than the rate limit thus set, we conclude that the binding in the ruthenium 2+ and 3+ states is the same. The decreases in C≡N stretching frequency on coordination to Ru(II) (compare MN and [2,MN,2], Table V) suggest that the nitrile groups constitute the binding sites. This is in accord with the measurements of E_f at least for DCA^- and TCM^- as ligands. The values are 0.15 and 0.30 V, respectively, to be compared to 0.426 V[22] for the $[(NH_3)_5RuNCCH_3]^{3+,2+}$ couple or to 0.57 V for the $[(NH_3)_5Ru(MN)]^{3+,2+}$ couple. The decrease in E_f when the nitriles are anionic is in accord with the expectation that negative charge will stabilize Ru(III) relative to Ru(II). Linkage isomerization involving a change from :N≡C to $:CR(CN)_2$ as a binding site for one of the ruthenium atoms, as already noted, may be a cause of some of the secondary reactions observed for the malononitrile derivatives, but these are rather slow changes.

The most notable observation made on the UV–visible absorption spectra is the very strong band registered in the visible region for Ru(III) when the ligand is anionic. For the mononuclear and binuclear ions with DCA as ligand, the bands appear at 420 and 400 nm, respectively. A shift to higher energies for the binuclear complex compared to that for the mononuclear complex is registered also for TCM, 599 and 562 nm, respectively. The absorptions in question are ascribable to ligand to metal charge transfer (LMCT), and thus the shifts to higher energy when two metal ions interact can be the results of their inductive effects. What is less expected is the shift to still higher energies observed for the mixed-valence complex based on TCM^- in the bridging ligand and for DCA^- as well (cf. Table III). This can be ascribed to the action of the πd orbitals of Ru(II) which lie above the π levels of the ligand and lower their energy. In the series MN^-, $EtMN^-$, or t-$BuMN^-$, LMCT absorption moves progressively to lower energies, consistent with the assignment made. For these as bridging groups the data unfortunately are less complete owing to the instability of some of the species. Good data are lacking for the $[3,L^-,2]$ systems, but it can be said that the absorption in the region in question does not differ markedly from that observed for the $[3,L^-,3]$ species.

Though the ligands used in this study are formally related, the effects of substitution in the middle position are so marked that within the series widely differing capacities to mediate the electronic interactions in the mixed-valence molecules are exhibited. This is hardly astonishing considering the effects of such substitution on properties such as the proton acidity. In the series NC–CH_2–CN, NC–CH(CN)–CN, NC–NH–CN, the pK_a for the first molecule is 11.2, while the last two $pK < 0$. Strong delocalization is indicated for the mixed-valence systems based on MN^-, $EtMN^-$, and t-$BuMN^-$ as bridging groups. Evidence in support is the intensity of the intervalence absorption for the mixed-valence species, $\epsilon > 10^4$ M^{-1} cm^{-1} (the highest on record for molecules based on Ru(III)–Ru(II), at least when the metal ions are widely separated), as well as the large value for the comproportionation constant. The near-IR band is much narrower[5] than that calculated by the Hush equation.[23] In other systems where on the basis of additional persuasive evidence we conclude that they approach the fully delocalized state,[1,2] the near-IR bands have also been found to be abnormally narrow. As has already been noted,[5] because the molecule is bent, the sensitivity of the near-IR band to solvent properties does not necessarily indicate trapping of charge by the solvent.

There is a progressive change in properties when the mixed-valence molecules based on t-$BuMN^-$ (or $EtMN^-$ or MN^-), TCM^-, and DCA^- are compared, which points to a progressive decrease in the extent of electron delocalization in that order. The separation in energy between the πd acceptor orbital and the π donor orbital decreases progressively as does the intensity of the LMCT band. This trend is expected when the stronger inductive effect of CN as compared to that of an alkyl group and the greater electronegativity of N compared to that of C are taken into account. The comproportionation constants decrease progressively—$K_{com} > 10^{10}$, 2.3×10^3, and $\sim 2 \times 10^2$. As has been mentioned, the width of the intervalence band at half-height for the t-$BuMN^-$-based species is much less than that calculated (2.12×10^3 cm^{-1} compared to 4.44×10^3 cm^{-1}). When TCM^- is the bridging ligand, the observed width is a few percent less than that calculated (3.7×10^3 vs. 3.9×10^3 cm^{-1}), and in $[3,DCA^-,2]$, the observed value is greater than that calculated (6.6×10^3 cm^{-1} compared to 4.6×10^3 cm^{-1}), the latter behavior being considered normal for valence trapped species.

The dominant mechanism for delocalization in the mixed-valence molecules based on MN^-, $EtMN^-$, and t-BuMN is undoubtedly delocalization from a carbon p orbital to the electron hole in the metal ion. The enormous enhancement in the acidity of the ligand attending the removal of one electron from [2,2] molecule indicates at once that electron density is removed in large part from the ligand. The ligands DCA^- and TCM^- are much more difficult to oxidize than is t-$BuMN^-$, for example. As judged by the criteria mentioned, delocalization is much less complete than for t-$BuMN^-$, in accord with the fact that the pπ electrons in these molecules are less susceptible to engagement by a proton or to removal by an oxidant. In these cases $d\pi-\pi^*$ delocalization becomes more prominent. For the DCA^--bridged species, it has been shown[6] that replacing some of the ammonia molecules by the electron-withdrawing ligands diminishes the coupling between the metal centers, a result that indicates that the dominant mechanism for delocalization is $d\pi-\pi^*$, despite the negative charge on the ligand.

Acknowledgment. Fellowship support for H.K. by CONICIT, Caracas, Venezuela, and support by the NSF (Grant No. GP-40829X) are gratefully acknowledged.

Registry No. $[Ru(NH_3)_5(TCM^-)](PF_6)_2$, 82917-48-4; $[(Ru(NH_3)_5)_2(TCM^-)](PF_6)_5$, 82917-50-8; $[Ru(NH_3)_5(MN^-)](PF_6)_2$, 82917-52-0; $[(Ru(NH_3)_5)_2(MN)](PF_6)_4$, 82917-54-2; $[(Ru(NH_3)_5)_2(MN^-)](PF_6)_5$, 82917-56-4; $[(Ru(NH_3)_5)_2(MN^-)]Br_5$, 82917-57-5; $[Ru(NH_3)_5(t\text{-}BuMN)](PF_6)_2$, 82917-59-7; $[(Ru(NH_3)_5)_2(t\text{-}BuMN)](PF_6)_4$, 60970-40-3; $[(Ru(NH_3)_5)_2(DBMN)](PF_6)_4$, 82917-61-1; $[(Ru(NH_3)_5)_2(BYMN)](PF_6)_4$, 82917-63-3; $[Ru(NH_3)_5Cl]Cl_2$, 18532-87-1; $[Ru(NH_3)_5OH_2](SO_3CF_3)_3$, 53195-18-9; $[Ru(NH_3)_5(DCA^-)](PF_6)$, 82917-65-5; $[(Ru(NH_3)_5)_2(DCA^-)](PF_6)_5$, 82917-66-6; $[(Ru(NH_3)_5)_2(DCA^-)]^{4+}$, 82978-73-2; $[(Ru(NH_3)_5)_2(DCA^-)](PF_6)_3$, 81572-54-5; $[Ru(NH_3)_5(TCM^-)]^+$, 82917-47-3; $[(Ru(NH_3)_5)_2(TCM^-)](PF_6)_4$, 83044-23-9; $[(Ru(NH_3)_5)_2(TCM^-)](PF_6)_3$, 82917-68-8; $[Ru(NH_3)_5(MN)]^{3+}$, 82917-69-9; $[Ru(NH_3)_5(MN)](PF_6)_2$, 82917-71-3; $[Ru(NH_3)_5(EtMN)]^{3+}$, 82932-61-4; $[Ru(NH_3)_5(EtMN)](PF_6)_2$, 82917-73-5; $[Ru(NH_3)_5(t\text{-}BuMN)](PF_6)_3$, 82917-75-7; $[(Ru(NH_3)_5)_2(DBMN)]^{6+}$, 82917-76-8; $[(Ru(NH_3)_5)_2(MN)]^{6+}$, 82917-77-9; $[(Ru(NH_3)_5)_2(MN)](PF_6)_5$, 83044-20-6; $[(Ru(NH_3)_5)_2(t\text{-}BuMN)]^{6+}$, 82917-78-0; $[(Ru(NH_3)_5)_2(t\text{-}BuMN)]^{5+}$, 82978-75-4; $[(Ru(NH_3)_5)_2(MN^-)]^{4+}$, 77305-45-4; $[(Ru(NH_3)_5)_2(t\text{-}BuMN^-)]^{3+}$, 82932-62-5; $[Ru(NH_3)_5(DBMN)](PF_6)_2$, 82917-81-5; $[(Ru(NH_3)_5)_2(EtMN)](PF_6)_4$, 82917-83-7; $[(Ru(NH_3)_5)_2(EtMN^-)](PF_6)_5$, 82917-85-9; $[Ru(NH_3)_5(t\text{-}BuMN^-)](PF_6)_2$, 82917-87-1; $[(Ru(NH_3)_5)_2(t\text{-}BuMN^-)](PF_6)_5$, 82917-89-3; $[(Ru(NH_3)_5)_2(t\text{-}BuMN^-)]^{4+}$, 60953-21-1; $[(Ru(NH_3)_5)_2(EtMN^-)]^{4+}$, 82978-74-3; $[(Ru(NH_3)_5)_2(DBMN)]^{5+}$, 82978-77-6; $[(NH_3)_5Ru(DCA^-)](PF_6)_2$, 81572-25-0; $Ru(NH_3)_6Cl_3$, 53293-35-9; $[(Ru(NH_3)_5)_2(DCA)](PF_6)_5$, 83044-19-3.

(22) Matsubara, T.; Ford, P. C. *Inorg. Chem.* **1976**, *15*, 1107.
(23) Hush, N. S. *Prog. Inorg. Chem.* **1971**, *8*, 391.